

Studies on Structural, Magnetic and Thermal Properties of $x\text{Fe}_2\text{TiO}_4-(1-x)\text{Fe}_3\text{O}_4$ ($0 \leq x \leq 1$) Pseudo-binary System

Monica Sorescu^{a,*}, Tianhong Xu^a, Adam Wise^b, Marina Díaz-Michelena^c, Michael E. McHenry^b

^a Department of Physics, Duquesne University, Fisher Hall, Pittsburgh, PA 15282, USA

^b Department of Materials Science and Engineering, Carnegie Mellon University, Roberts Hall, Pittsburgh, PA 15213, USA

^c Space Programs and Space Sciences Department, Instituto Nacional de Técnica Aeroespacial (INTA), Madrid 28850, Spain

ARTICLE INFO

Article history:

Received 18 August 2011

Received in revised form

15 November 2011

Available online 9 December 2011

Keywords:

Titanomagnetite

Mars

X-ray powder diffraction

Mössbauer spectroscopy

Simultaneous DSC–TGA

ABSTRACT

The $x\text{Fe}_2\text{TiO}_4-(1-x)\text{Fe}_3\text{O}_4$ pseudo-binary systems ($0 \leq x \leq 1$) of ulvöspinel component were synthesized by solid-state reaction between ulvöspinel Fe_2TiO_4 precursors and commercial Fe_3O_4 powders in stoichiometric proportions. Crystalline structures were determined by X-ray powder diffraction (XRD) and it was found that the as-obtained titanomagnetites maintain an inverse spinel structure. The lattice parameter a of synthesized titanomagnetite increases linearly with the increase in the ulvöspinel component. ^{57}Fe room temperature Mössbauer spectra were employed to evaluate the magnetic properties and cation distribution. The hyperfine magnetic field is observed to decrease with increasing Fe_2TiO_4 component. The fraction of Fe^{2+} in both tetrahedral and octahedral sites increases with the increase in Ti^{4+} content, due to the substitution and reduction of Fe^{3+} by Ti^{4+} that maintains the charge balance in the spinel structure. For x in the range of $0 \leq x \leq 0.4$, the solid solution is ferrimagnetic at room temperature. However, it shows weak ferrimagnetic and paramagnetic behavior for x in the range of $0.4 < x \leq 0.7$. When $x > 0.70$, it only shows paramagnetic behavior, with the appearance of quadrupole doublets in the Mössbauer spectra. Simultaneous differential scanning calorimetry and thermogravimetric analysis (DSC–TGA) studies showed that magnetite is not stable, and thermal decomposition of magnetite occurs with weight losses accompanying with exothermic processes under heat treatment in inert atmosphere.

© 2011 Elsevier B.V. All rights reserved.

1. Introduction

In basalts, Fe–Ti spinels (titanomagnetite) are the carriers of the natural remanent magnetization of Mars. Studies of the magnetic properties of such rocks have provided a wealth of information on the magnetic history of Mars. The further studies of planetary magnetism provide insight into the validity of various models of geological evolution of planets and satellites and thus of the Solar System. The Mars Global Surveyor mission's results showed the first unambiguous measurements of the magnetic field on Mars [1]. These results showed that Mars presently has no active geological dynamo and its global magnetic field is of crustal origin even though studies of Martian meteorites indicate that fields as large as 3000 nT may have once existed on the surface of Mars. Mappings of the Martian magnetic field reveal anomalous regions of intense magnetization [2] distributed in “stripes” of alternating polarity.

Important components among the abundant mineral types on the Mars are ferrites and titanomagnetites, and those materials usually contain medium Ti content. Due to their abundance on the Martian surface, studying the formation of $x\text{Fe}_2\text{TiO}_4-(1-x)\text{Fe}_3\text{O}_4$ solid solutions with different amounts of Ti content and their magnetic properties may be important in understanding the geomagnetism of Mars. In order to explain the remanent magnetic state on Mars it is necessary to postulate abundant materials with large remanent magnetization. This in turn requires monodomain magnets, with sufficiently large Neel temperatures with sufficient pinning of the remanent state to avoid thermally activated switching. Spinodal decomposition in an asymmetric miscibility gap in the titanomagnetite system can explain these features [3,4].

Titanomagnetites are solid solutions of magnetite and ulvöspinel (Fe_2TiO_4), in which a fraction of Fe^{3+} ions on the octahedral sites of magnetite are substituted by Ti^{4+} ions. When a Fe^{3+} is substituted by a Ti^{4+} ion, a Fe^{3+} ion on either tetrahedral or octahedral site must convert to a Fe^{2+} in order to maintain charge balance. It has been reported that Ti^{4+} ions have strong preference for octahedral sites in the titanomagnetites [5]. However, occupation of Ti^{4+} ions on tetrahedral sites was also found to be a

* Corresponding author. Tel.: +1 412 396 4166; fax: +1 412 396 4829.
E-mail address: sorescu@duq.edu (M. Sorescu).

possible choice in Fe–Ni–Ti, Li–Mn–Ti and Li–Cr–Ti spinels [6–8]. The ordering of these cations is still uncertain; depending on the molar fraction x and cation distribution on the tetrahedral and octahedral sites, the solid solutions $x\text{Fe}_2\text{TiO}_4-(1-x)\text{Fe}_3\text{O}_4$ can exhibit ferrimagnetic, antiferromagnetic, spin glass and paramagnetic behaviors with different Ti^{4+} contents.

Mössbauer spectroscopy has proved to be a valuable tool in geology giving information about various aspects of iron mineralogy that in turn can provide insight into the magnetic history of minerals on the Mars. Recently, the cation distributions in titanomagnetites have been widely investigated, and several models have been proposed to describe the Fe^{3+} ions on tetrahedral and octahedral sites as a function of Ti content [9–13]. So far, eight models were used to describe the relationship between cation distribution and molar fraction of ulvöspinel component [14]. However, these models are based on the saturation magnetization measurements performed at low temperature such as 77 K or Mössbauer spectroscopy measurements at 4.2 K under strong external magnetic field, and the de-convolution of the Fe^{3+} sextet on the tetrahedral and octahedral sites is not completely effective and conclusive. Recently, X-ray magnetic circular dichroism (XMCD) was also employed to study the Fe site occupancy in magnetite-ulvöspinel solid solutions, while this technique is only suited to probe the surface with a depth of ~ 4.5 nm [14]. To the best of our knowledge, no cation distribution in titanomagnetite has been successfully investigated by room temperature Mössbauer spectroscopy without strong external magnetic field.

Recently, thermal analysis was employed to study the oxidation behavior of titanomagnetite powders [15–17]. However, those experiments were only conducted under oxidation atmosphere to study the oxidation behavior of Fe^{2+} either located in octahedral B or tetrahedral A sites. No thermal behavior of the $x\text{Fe}_2\text{TiO}_4-(1-x)\text{Fe}_3\text{O}_4$ pseudo-binary systems under inert atmosphere has been studied. The simultaneous DSC–TGA investigation under inert atmosphere on the solid solution systems may provide some useful information about the formation process of titanomagnetite.

This work reports the successful synthesis of solid solutions $x\text{Fe}_2\text{TiO}_4-(1-x)\text{Fe}_3\text{O}_4$ in whole ranges with $0 \leq x \leq 1$ by use of the solid state reaction. The solid state reactions between synthesized Fe_2TiO_4 and commercial Fe_3O_4 powders were performed in similar conditions as expected to occur in Martian crust. Magnetic properties of these as-obtained materials were investigated through room temperature Mössbauer spectroscopy. The variations in magnetic properties of the solid solution as a function of Fe_2TiO_4 molar fraction x were investigated, and the Fe cation distribution in tetrahedral and octahedral sites was derived from the overall oxidation state of Fe ions on the tetrahedral site. The thermal behavior of as-obtained solid solutions under inert atmosphere, which depends on the Fe_2TiO_4 component, was also reported. These are important for future interpretation of magnetic and structural data collected on Mars.

2. Experimental

The $x\text{Fe}_2\text{TiO}_4-(1-x)\text{Fe}_3\text{O}_4$ ($0 \leq x \leq 1$) series were produced by solid state synthesis. Fe_2TiO_4 was prepared from Fe_2O_3 and TiO_2 mixed in stoichiometric proportions with 5.4% excess Fe sponge. Components were ground with a mortar and pestle, pressed into pellets, loaded into Fe crucibles and heated to 1050 °C for 60 h in an Ar atmosphere to prevent oxidation.

The Fe_2TiO_4 precursor pellets were SPEX ball-milled to produce powders of an appropriate size for mixing with commercial Fe_3O_4 powder. This ball-milled Fe_2TiO_4 powder was mixed with

commercial Fe_3O_4 powder in different proportions to produce the series studied here. Each composition was ball-milled for another 10 min to reduce the particle size and homogenize the powder mixture, and then pressed into pellets of 0.5 in in diameter and ~ 0.15 in thick. The pellets were placed in 1010 steel crucibles into an Ar furnace at 950 °C for a bake of 60 h. Pellets were cooled in furnace under the Ar atmosphere to 400 °C, then removed to air-cool to room temperature.

The as-synthesized $\text{Fe}_2\text{TiO}_4\text{--Fe}_3\text{O}_4$ solid solutions were powdered for phase, magnetic and thermal examinations. The X-ray powder diffraction (XRD) patterns of the solid solutions were obtained using a PANalytic X'Pert Pro MPO diffractometer with CuK_α radiation (45 kV/40 mA, $\lambda = 1.54187 \text{ \AA}$) with a nickel filter on the diffracted side. A silicon-strip detector called X'cellerator was used. The scanning range was 10–80° (2θ) with a step size of 0.02°.

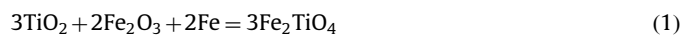
Room temperature transmission Mössbauer spectra were recorded using a MS-1200 constant acceleration spectrometer with a 10 mCi ^{57}Co source diffused in Rh matrix. Least-squares fittings of the Mössbauer spectra were performed with the NORMOS program.

Simultaneous DSC–TGA experiments were performed using a Netzsch Model STA 449 F3 Jupiter instrument with a Silicon Carbide (SiC) furnace. Samples were contained in an alumina crucible with an alumina lid. Series of experiments were performed using 20 ± 2 mg sample size. The atmosphere consisted of flowing protective argon gas at a rate of 50 ml/min. DSC and TGA curves were obtained by heating samples from room temperature to 800 °C with a ramp rate of 10 °C/min. Both DSC and TGA curves were corrected by subtraction of a baseline which was run under identical conditions as the DSC–TGA measurement with residue of samples in the crucible. The Netzsch Proteus Thermal Analysis software was used for DSC and TGA data analysis.

3. Results and Discussion

3.1. X-ray Powder Diffraction

Fig. 1 shows the X-ray powder diffraction of the $x\text{Fe}_2\text{TiO}_4-(1-x)\text{Fe}_3\text{O}_4$ with different Fe_2TiO_4 molar fractions x in the range of $0 \leq x \leq 1$. As expected, Fig. 1a is a typical powder diffraction pattern of single-phase cubic spinel magnetite. The XRD of the synthesized Fe_2TiO_4 materials was shown in Fig. 1g, and verified to be the spinel phase along with less than 3% impurity of ilmenite (FeTiO_3) phase, which is a typical phase approaching ulvöspinel. The Fe_2TiO_4 spinel phase forms according to the reaction



The XRD patterns show that the synthesized $x\text{Fe}_2\text{TiO}_4-(1-x)\text{Fe}_3\text{O}_4$ solid solutions with $x = 0.4, 0.6, 0.7$ and 0.75 are cubic spinels. Absence of any other phases confirms that a complete solid solution has been formed between Fe_3O_4 and Fe_2TiO_4 , except for $x = 0.6$, where traces of FeO were detected. However, for $x = 0.65$, a pure spinel cubic phase was not achieved (Fig. 1d). Other phases, such as Fe_2O_3 , Fe_2TiO_5 and FeTiO_3 , were detected along with the spinel structure, suggesting that this molar fraction may not be suitable to obtain the solid solution with single-phase of cubic spinel. The detected three side phases may also result from exsolution when the formed solid solution becomes unstable under cooling process, and early spinodal decomposition occurs [3]. It has been generally reported that the miscibility gap in the $\text{Fe}_2\text{TiO}_4\text{--Fe}_3\text{O}_4$ solid solution series leads to the development of exsolution intergrowths in titanomagnetites of intermediate composition [18,19], and the spinodal

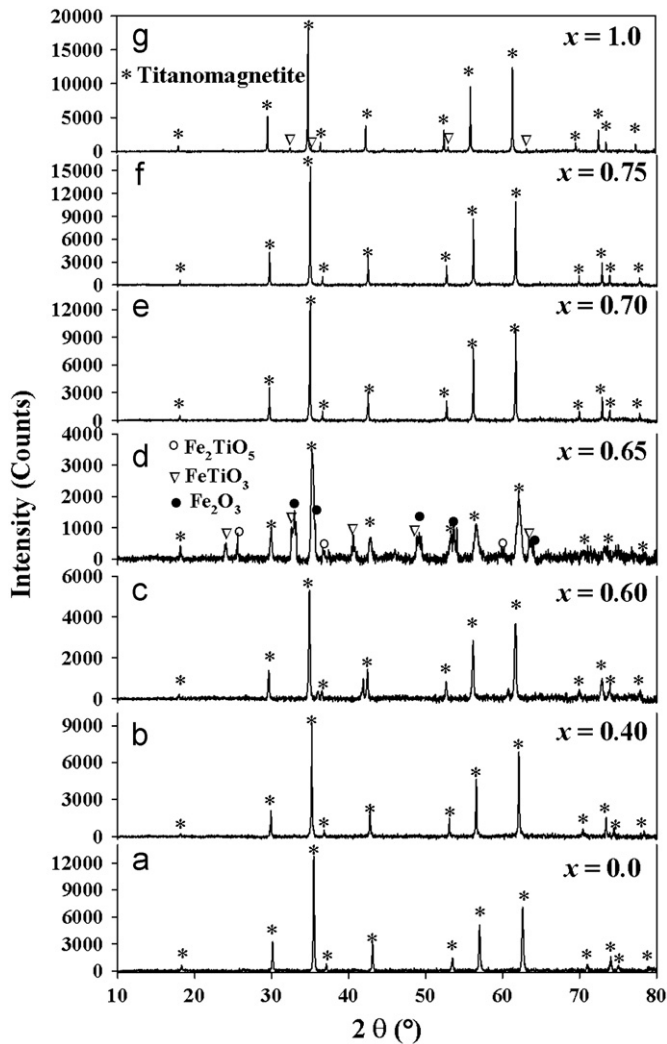


Fig. 1. XRD patterns of the $x\text{Fe}_2\text{TiO}_4-(1-x)\text{Fe}_3\text{O}_4$ ($0 \leq x \leq 1$) pseudo-binary system with molar fraction x (a) $x=0.0$, (b) $x=0.4$, (c) $x=0.6$, (d) $x=0.65$, (e) $x=0.70$, (f) $x=0.75$ and (g) $x=1.0$.

decomposition in titanomagnetite was also observed from the electron microscopy studies [2,20]. This asymmetry in the miscibility gap is not predicted from regular solution theory and must be further understood in the future. However, the X-ray powder diffraction peaks of Fe_3O_4 from spinodal decomposition were not observed, probably due to the strong overlap in diffraction peaks between the Fe_3O_4 and the as-obtained Ti-rich spinel structures. The broadening of the XRD peaks is consistent with a fine microstructure characteristic of spinodal decomposition.

Compared to the XRD patterns of the as-obtained spinel materials, it was found that the diffraction peaks shift to lower 2θ angles systematically with the increase in the molar fraction x of Fe_2TiO_4 , owing to the difference in radius between $\text{Fe}^{3+}/\text{Fe}^{2+}$ and Ti^{4+} . The increase in the lattice parameter a of the as-obtained spinel materials with the increase in the Ti^{4+} content is also suggested. Fig. 2 shows variation of the lattice parameter a , which was extracted from the Rietveld structural refinement of the XRD patterns, as a function of the Fe_2TiO_4 molar fraction x . It was found that there is a linear relationship between a and x , a increases from 8.3894 Å to 8.5410 Å for $x=0$ and $x=1$, respectively. The linear relationship follows the Vegard's rule [21,22], such that the lattice parameter a of the formed solid solution has a weighted average of that of the two end members [23]. It has to be noted that the lattice parameter a of the solid solution with

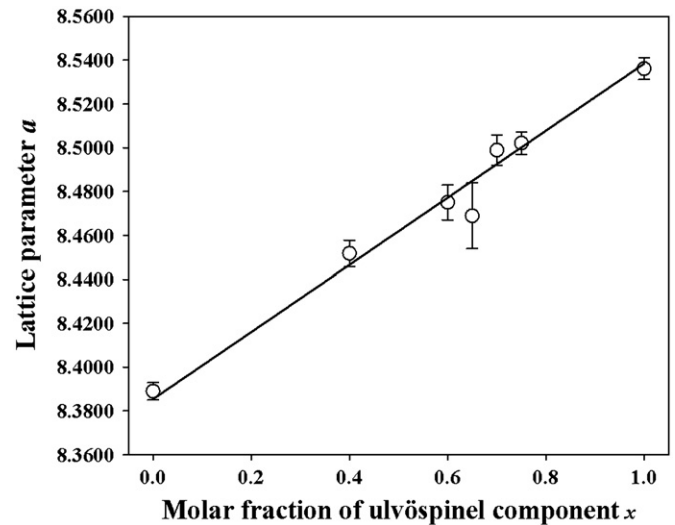


Fig. 2. Lattice parameter a of the $x\text{Fe}_2\text{TiO}_4-(1-x)\text{Fe}_3\text{O}_4$ ($0 \leq x \leq 1$) pseudo-binary system as a function of the Fe_2TiO_4 molar fraction of x .

$x=0.65$ is off the curve to some extent, consistent with the measurable amounts of hematite, Fe_2TiO_5 , FeTiO_3 impurities and possible magnetite phase, respectively. The relationship between lattice parameter a and Fe_2TiO_4 content is similar to that reported in the literatures with S-shape curve; the small difference may arise from the different preparation methods and the formation of a non-stoichiometric solid solution [24,25]. The decrease in the relative amount of Fe_3O_4 and increasing Fe_2TiO_4 content results in a larger lattice parameter a of the solid solution $x\text{Fe}_2\text{TiO}_4-(1-x)\text{Fe}_3\text{O}_4$. The linear change in lattice parameter a is induced by the Ti substitution of Fe ions and the reduction of Fe^{3+} to maintain charge balance in the formed solid solutions.

The spinel structure has a space group of $Fd3m$. This space group requires equivalence among tetrahedral sites and among octahedral sites. For spinel with different types of cations occurring together at the same sites, a random distribution of the cations over equivalent sites is required, otherwise the symmetry will be reduced if such equivalent site is violated and the cations order in various ways [24]. All of the XRD patterns are consistent with the $Fd3m$ space group, no extra reflection and splitting of spinel peak was observed, indicating the Ti^{4+} cations are randomly distributed in the formed solid solutions with different molar fraction x of ulvöspinel component.

3.2. Mössbauer Spectroscopy

Both magnetite and ulvöspinel have a cubic inverse spinel structure, with the structure formula of $(\text{Fe}^{3+})[\text{Fe}^{2+}\text{Fe}^{3+}]\text{O}_4$ and $(\text{Fe}^{2+})[\text{Fe}^{2+}\text{Ti}^{4+}]\text{O}_4$, respectively. The round bracket stands for tetrahedral site and square bracket for octahedral site, respectively. Cation distribution in solid solution titanomagnetites is essential to understand the complicated magnetic behavior of these minerals with remanent magnetism in rocks, which includes the magnetocrystalline anisotropy and spin canting [13]. The substitution of non-magnetic Ti^{4+} can have similar effects to the substitution of non-magnetic Al^{3+} [26] and Zn^{2+} in Ni–Zn ferrites [27,28]. The preferential breaking of A–B superexchange bonds can stabilize Yafet–Kittel triangular spin structures causing dipole moments to have to switch against stronger exchange interactions. This manifests itself in non-saturating magnetization curves up to large fields [4,26] causing difficulty inferring cation occupancies from saturation magnetizations. Magnetic behavior can further be complicated by spatially

inhomogeneous cation distributions caused by spinodal decomposition [29] or diffusion for surfaces or interfaces [28].

The three Mössbauer parameters, namely isomer shift (I.S., relative to α -Fe), quadrupole shift/splitting (Q.S.) and hyperfine magnetic field (B), can provide important information about a particular compound with an atomic resolution scale. Especially, the isomer shift provides direct information about the electron density at nucleus.

Magnetite (Fe_3O_4) is an oxide with the inverse spinel structure, which has one Fe^{3+} ion on the tetrahedral site and two Fe ions, with a total oxidation state of +5, on the octahedral site. Fig. 3a shows the room temperature Mössbauer spectrum of magnetite. It could be resolved by considering two Zeeman sextets (Table 1), corresponding to the two magnetic sublattices present in the sample. The tetrahedral site is represented by a sextet with a magnetic hyperfine field of 49.22 T and isomer shift of 0.059 mm/s, while the octahedral site is described by a six-line pattern having a hyperfine magnetic field of 46.20 T and isomer shift of 0.472 mm/s. Lowering of the hyperfine magnetic field value of the second sublattice is related to the presence of Fe^{2+} ions at the octahedral sites. The site populations of the tetrahedral and the octahedral

Table 1

Mössbauer parameters for the $x\text{Fe}_2\text{TiO}_4-(1-x)\text{Fe}_3\text{O}_4$ ($0.0 \leq x \leq 1$) pseudo-binary system.

x	I.S. (δ , mm/s)	Q.S. (mm/s)	B (T)	Abundance (%)
$x=0.0$	0.059	0.024	49.22	34.6
	0.472	0.047	46.20	65.4
$x=0.40$	0.191	-0.039	46.75	27.7
	0.071	0.360	44.29	11.1
	0.550	-0.155	41.99	30.6
	0.489	-0.222	36.71	30.6
$x=0.60$	0.318	0.076	38.45	29.0
	0.341	0.088	33.25	11.8
	0.417	-0.022	27.63	33.2
	0.700	0.778	/	26.0
$x=0.65$	0.231	-0.012	50.71	12.8
	0.332	-0.082	46.80	22.8
	0.360	0.044	44.19	6.7
	0.470	0.176	40.72	42.0
$x=0.70$	0.252	0.558	/	15.7
	0.332	0.033	27.83	33.4
	0.373	0.072	22.22	9.8
	0.387	-0.150	19.48	36.5
$x=0.75$	0.753	1.211	/	20.3
	0.772	2.188	/	8.1
	0.768	1.378	/	38.9
	0.793	1.680	/	53.0
$x=1.0$	0.904	1.223	/	50.3
	0.903	1.976	/	49.7
Error	± 0.01	± 0.02	± 1.00	± 0.5

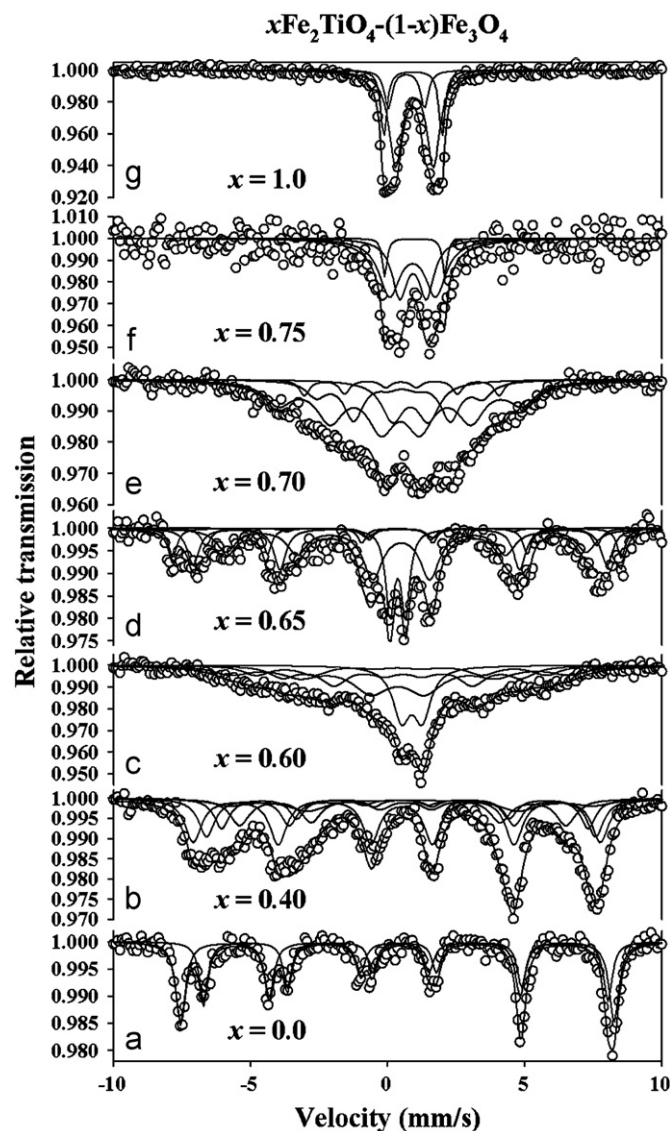


Fig. 3. Mössbauer spectra of the $x\text{Fe}_2\text{TiO}_4-(1-x)\text{Fe}_3\text{O}_4$ ($0 \leq x \leq 1$) pseudo-binary system with molar fraction x (a) $x=0.0$, (b) $x=0.4$, (c) $x=0.6$, (d) $x=0.65$, (e) $x=0.70$, (f) $x=0.75$ and (g) $x=1.0$.

sites are 34.6% and 65.4%, respectively. The ratio of the population of Fe ions on tetrahedral and octahedral sites is close to the theoretical value of 1:2, indicating a high degree of stoichiometry of the initial magnetite material [30]. The spectrum also indicates that magnetite does not contain any Fe^{2+} in tetrahedral sites, while it contains both Fe^{3+} and Fe^{2+} in octahedral sites. As an equal number of Fe^{3+} and Fe^{2+} are present at octahedral sites, an average oxidation state of +2.5 can be assumed for Fe ions in octahedral sites, due to the electron hopping between Fe^{3+} and Fe^{2+} .

Fig. 3g shows the room temperature Mössbauer spectrum of the as-synthesized Fe_2TiO_4 . The spectrum of Fe_2TiO_4 is very different from that of magnetite; instead of two sextets, only one broad doublet is visible. The least-square fitting shows that the broad doublet is composed of two quadrupole doublets. The corresponding values of isomer shift (~ 0.90 mm/s) and quadrupole splitting ($1.2 \leq \text{Q.S.} \leq 2.0$ mm/s) for these two doublets are much larger than those of Fe^{3+} on the tetrahedral site and $\text{Fe}^{2.5+}$ on the octahedral site of magnetite, indicating that Fe ions exist only as Fe^{2+} ions in the spinel Fe_2TiO_4 . This is in good agreement with the charge balance, which implies that Ti ions exist as Ti^{4+} and Fe ions exist as Fe^{2+} . Though a very small portion of impurities of FeTiO_3 was detected from XRD measurement, the contribution of FeTiO_3 to the overall magnetic properties is also from Fe^{2+} ions. On the other hand, the percentage of FeTiO_3 was found to be less than 3%, therefore, the two doublets can be mainly considered from the contribution of Fe^{2+} in Fe_2TiO_4 . The two doublets in the Mössbauer spectrum of Fe_2TiO_4 can be explained in terms of the Fe^{2+} ions on both tetrahedral site and octahedral sites [31]. The percentage of these two doublets from least-square fitting follows the almost equal distribution of Fe^{2+} ions on the tetrahedral (Q.S.=1.223 mm/s) and octahedral (Q.S.=1.976 mm/s) sites, with the percentage of 50.3% and 49.7%, respectively. The existence of small different percentages is reasonable since the field gradient values at the Fe^{2+} ions are different because of the partial inversion of the synthesized crystal as suggested from Tanaka et al. [32,33] or by other structural reasons, such as vacancies in the neighborhood and impurities. The almost equal amount of Fe^{2+} on tetrahedral and

octahedral site also suggests that Ti^{4+} ions are located on the octahedral site of Fe_2TiO_4 . It was also reported by Vanleerberghe and Vandenberghe [34] that no crystallographic ordering between Ti^{4+} and Fe^{2+} ions on octahedral site was observed, which results in a whole range of possible distributions of the Fe^{2+} surroundings and gives rise to distributions in the quadrupole interaction for both sites. Therefore, it is not surprising to find only one paramagnetic broad doublet spectra as shown in Fig. 3g. Only one broad doublet is observed for the synthesized Fe_2TiO_4 sample, suggesting it is paramagnetic at room temperature, which is in good agreement with the reported results that Fe_2TiO_4 is paramagnetic at room temperature and antiferromagnetic at very low temperature [35]. From the above Mössbauer analysis of magnetite and Fe_2TiO_4 , the cation distribution is well established for these two end members. In order to determine the cation distribution in solid solution $xFe_2TiO_4-(1-x)Fe_3O_4$ with different x values, the room temperature Mössbauer spectra were also recorded.

Fig. 3b shows the transmission Mössbauer spectrum of the solid solution $xFe_2TiO_4-(1-x)Fe_3O_4$ with $x=0.4$, corresponding to $Fe_{2.6}Ti_{0.4}O_4$. Compared to the magnetic properties of original magnetite and Fe_2TiO_4 samples, the formed solid solution showed completely different magnetic properties, though it still maintains the spinel structure, as identified from XRD measurement. Local variations in hyperfine fields produce broad lines in the Mössbauer spectrum. Least-square fitting shows that the Mössbauer spectrum for this sample is composed of superimposed four magnetic hyperfine sextets, and the overall hyperfine magnetic field decreases with the introduction of Fe_2TiO_4 , with the values of 46.75, 44.29, 41.99 and 36.71 T, respectively. The two sextets, with the hyperfine magnetic fields of 46.75 and 44.29 T, respectively, can be assigned to Fe ions on tetrahedral sites. The other two sextets with hyperfine field of 41.99 and 36.71 T can be assigned to Fe ions on octahedral sites. The isomer shift of Fe ion on tetrahedral site is smaller than that on octahedral site. Population of Fe ions on the tetrahedral sites, in other words, the sum of the two sextets with higher magnetic fields, is about 38.8%, which is very close to the theoretical value of 38.45% as calculated from the $(Fe_1)[Fe_{1.6}Ti_{0.4}]O_4$ formula, suggesting that Ti^{4+} remains at octahedral site. This is consistent with Mössbauer result of Fe_2TiO_4 that Ti^{4+} occupies octahedral sites. Similar to the Mössbauer spectrum of Fe_3O_4 , the rapid electron hopping between Fe^{2+} and Fe^{3+} on the octahedral sites makes it very difficult to completely separate the Fe^{2+} and Fe^{3+} cations on octahedral sites, although the spectrum can be fitted with two sextets with smaller hyperfine magnetic fields. The existence of two sextets for Fe ion on tetrahedral site suggests that part of Fe^{3+} was reduced as well, with the sign of decrease in the strength of hyperfine magnetic field and increase in isomer shift, respectively. The Mössbauer result shows the cation distribution in this synthesized solid solution is following the model reported by O'Reilly et al [11]. The hyperfine magnetic field strength as a function of Ti content ($0 \leq x \leq 0.5$) was also studied by use of room temperature Mössbauer spectra [36–38] and it was reported that the outer sextet of the $xFe_2TiO_4-(1-x)Fe_3O_4$ solid solution with $x=0.4$ has a hyperfine magnetic field of 45.5 T; our results are in great agreement with the reported values.

Fig. 3c shows the transmission Mössbauer spectrum of the solid solution $xFe_2TiO_4-(1-x)Fe_3O_4$ with $x=0.6$, corresponding to $Fe_{2.4}Ti_{0.6}O_4$. Similar to that of $x=0.4$, the formed solid solution showed completely different magnetic properties from those of original magnetite and Fe_2TiO_4 samples. The Mössbauer spectrum is composed of three superimposed magnetic hyperfine sextets and one doublet. The corresponding hyperfine magnetic fields for the sextets are 38.45, 33.25 and 27.63 T, respectively, with areal percentages of 29.0%, 11.8%, 33.2%, respectively. The two sextets,

with the highest hyperfine magnetic fields of 38.45 T and 33.25 T, can be assigned to Fe ions on tetrahedral sites. The percentage of Fe ions on the tetrahedral sites is the sum of the populations of Fe ions with higher hyperfine magnetic fields, which is about 40.8% and very close to the theoretical value of 41.66% as calculated from the $(Fe_1)[Fe_{1.4}Ti_{0.6}]O_4$ formula. The other sextet can be assigned to Fe ions on octahedral sites. The decrease in the hyperfine field strength of Fe ions located on tetrahedral sites suggests that part of Fe^{3+} ions were reduced due to the substitution between Ti^{4+} and Fe ions. The doublet has a population of 26.0%, and with isomer shift and quadrupole splitting values of 0.700 and 0.778 mm/s, which can be assigned to Fe ions on octahedral sites. The appearance of the quadrupole splitting doublet suggests that more Fe^{3+} ions are reduced by the introduction of more Ti^{4+} into the solid solutions.

Fig. 3d shows the transmission Mössbauer spectrum of the solid solution $xFe_2TiO_4-(1-x)Fe_3O_4$ with $x=0.65$, corresponding to $Fe_{2.35}Ti_{0.65}O_4$. The Mössbauer spectrum is composed of superimposed four magnetic hyperfine sextets and one doublet. The corresponding hyperfine magnetic fields for the sextets are 50.71, 46.80, 44.19 and 40.72 T, respectively, with areal percentages of 12.8%, 22.8%, 6.7% and 42.0%, respectively. The presence of measurable amounts of hematite, $FeTiO_3$ and Fe_2TiO_5 also makes it more difficult to quantify the Fe cation distribution on tetrahedral and octahedral sites.

Fig. 3e shows the transmission Mössbauer spectrum of the solid solution $xFe_2TiO_4-(1-x)Fe_3O_4$ with $x=0.7$, corresponding to $Fe_{2.3}Ti_{0.7}O_4$. The Mössbauer spectrum is composed of three superimposed magnetic hyperfine sextets and one doublet. The corresponding hyperfine magnetic fields for the three sextets are 27.83, 22.22 and 19.48 T, respectively, with areal percentages of 33.4%, 9.8%, 36.5%, respectively. Compared to the solid solution $xFe_2TiO_4-(1-x)Fe_3O_4$ with $x=0.6$ and 0.4, the hyperfine magnetic field strengths were found to be dramatically smaller. The sextets with the two highest hyperfine magnetic fields of 27.83 T and 22.22 T, and isomer shifts of 0.332 and 0.373 mm/s, respectively, can be assigned to Fe ions on tetrahedral site. The other sextet and the doublet can be assigned to Fe ions on B sites. The percentage of Fe ion on the tetrahedral site is about 43.2%, which is very close to the ideal spinel structure and theoretical value of 43.38% as calculated from the $(Fe_1)[Fe_{1.3}Ti_{0.7}]O_4$ formula. Furthermore, this also suggests that Ti^{4+} remains on the octahedral site. However, some of Fe^{3+} ions on tetrahedral site are reduced, which results in a much smaller hyperfine magnetic field strength. Analysis of the values of isomer shift and quadrupole splitting of the doublet, with the value of 0.753 and 1.211 mm/s, suggests Fe ions are further reduced to Fe^{2+} on octahedral site at this Ti^{4+} content. In order to keep the charge balance in the spinel structure, the percentage of Fe ions with the reduced oxidation state increases with the increase in the molar fraction x of Fe_2TiO_4 , which can be confirmed from the increase in areal percentage of the doublet.

Fig. 3f shows the room temperature Mössbauer spectrum of the solid solution $xFe_2TiO_4-(1-x)Fe_3O_4$ with $x=0.75$, corresponding to $Fe_{2.25}Ti_{0.75}O_4$. Different from other samples and similar to the Fe_2TiO_4 , the Mössbauer spectrum of the solid solution is composed of one broad asymmetric doublet, which can be deconvoluted to three doublets, and with areal percentages of 8.1%, 38.9%, 53.0%, respectively; no sextet was observed. Analysis of the values of isomer shift and quadrupole splitting of the doublets can determine the Fe cation distribution on tetrahedral site and octahedral site. The doublets with the isomer shift values of 0.772 mm/s and 0.768 mm/s can be assigned to Fe ions located on tetrahedral site, with a population of 47.0%, close to the theoretical value (44.44%) with formula of $(Fe_1)[Fe_{1.25}Ti_{0.75}]O_4$. The other doublet, with isomer shift and quadrupole splitting values of 0.793 and 1.680 mm/s can be assigned to Fe ions on octahedral

sites. Considering this Fe_2TiO_4 molar fraction of $x=0.75$ and the charge balance in the spinel structures, some portion of Fe ions on tetrahedral sites should still maintain Fe^{3+} character. However, no sextet corresponding to Fe^{3+} on tetrahedral site was observed. Most of the Fe ions exist as Fe^{2+} on tetrahedral sites and some are Fe^{3+} , however, the solid solution only shows paramagnetic behavior at room temperature, indicating rapid electron hopping between Fe^{2+} and Fe^{3+} ions on tetrahedral site as well. The paramagnetic properties are probably due to the dominating amount of Fe^{2+} ions in the solid solution $x\text{Fe}_2\text{TiO}_4-(1-x)\text{Fe}_3\text{O}_4$ with molar fraction $x=0.75$. Similar paramagnetic behavior was also observed for samples with $x=0.80, 0.85, 0.90$, respectively. The slight asymmetry of the broad quadrupole splitting doublet is attributed to the contribution of Fe^{3+} on the tetrahedral site [39,40].

Progressive substitution of iron by titanium in titanomagnetite solid solution shows that the ratio of $\text{Fe}^{3+}/\text{Fe}^{2+}$ decreases; the decrease in the hyperfine magnetic field strength can be described by the classic substitution between Fe^{3+} and Ti^{4+} as a consequence of Fe^{3+} reduction:



According to the Mössbauer spectra, the $x\text{Fe}_2\text{TiO}_4-(1-x)\text{Fe}_3\text{O}_4$ pseudo-binary solid solutions can be divided into three types with different magnetic properties: for $0 \leq x \leq 0.4$, the solid solution shows ferrimagnetic behavior, and the Mössbauer spectra can be de-convoluted as sextets; for $0.4 < x \leq 0.7$, the solid solution shows both weak ferrimagnetic and paramagnetic behaviors, with dramatic decrease in hyperfine magnetic field strength of sextets and appearance of quadrupole-split doublet; for $0.7 < x \leq 1$, the solid solution only shows paramagnetic behavior and the Mössbauer spectra consist of quadrupole-split doublets only. The difference in magnetic properties arises from the degree of classic substitution between Ti and Fe ions and cation distribution on tetrahedral/octahedral sites.

For the cation distribution in the $x\text{Fe}_2\text{TiO}_4-(1-x)\text{Fe}_3\text{O}_4$ solid solution, it is widely believed that Ti^{4+} prefers the octahedral site, which is confirmed by our room temperature Mössbauer results that the population percentages of Fe ions on the tetrahedral and octahedral sites are extremely close to the theoretical value calculated from the theoretical formula. Though the percentage of Fe ions on tetrahedral and octahedral site can be determined as mentioned previously, however, one cannot derive the Fe^{3+} and Fe^{2+} cation distribution in tetrahedral and octahedral sites directly from the room temperature Mössbauer spectra due to the coexistence of Fe^{3+} and Fe^{2+} and electron hopping. The area percentages of de-convoluted sextets and doublets cannot be used to calculate the Fe^{3+} and Fe^{2+} atomic numbers on tetrahedral and octahedral sites per solid solution formula, owing to the strong overlaps between these sub-spectra. However, by the analysis of isomer shift values of Fe^{3+} on tetrahedral site in magnetite, $\text{Fe}^{2.5+}$ on octahedral site in magnetite, and Fe^{2+} on either tetrahedral or octahedral sites in the synthesized Fe_2TiO_4 , respectively, it is very interesting to observe that there is a linear relationship between the oxidation state of Fe ion and the corresponding isomer shift, which is shown in Fig. 4.

Isomer shift is a relative measure describing a shift in the resonance energy of a nucleus due to the transition of electrons within its s orbital. The whole spectrum is shifted in either a positive or negative direction depending upon the s electron charge density. This change arises due to alterations in the electrostatic response between the non-zero probability s orbital electrons and the non-zero volume nucleus orbit. Only electrons in s orbital demonstrate non-zero probability, because their 3D spherical shape incorporates the volume taken up by the nucleus. In other words, the s electron density is largely affected by the

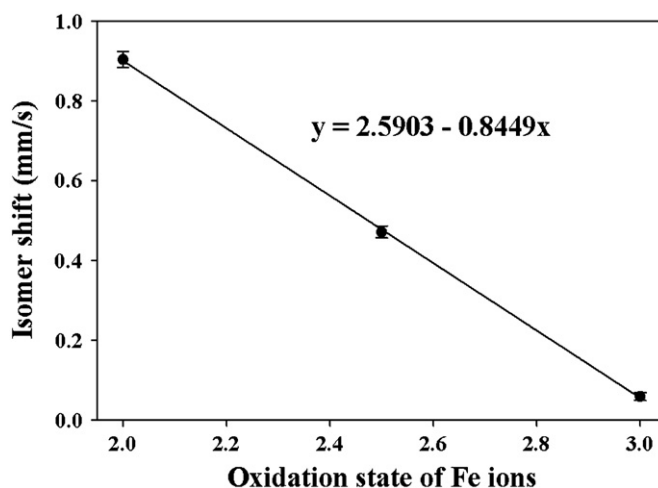


Fig. 4. Plot of oxidation state of Fe ions in magnetite and ulvöspinel Fe_2TiO_4 as a function of isomer shift extracted from the corresponding fitted Mössbauer spectrum.

oxidation state, though it is also affected by the chemical environment of the atom to some extent [41].

Due to the existence of linear relationship of oxidation state of Fe ion and the corresponding isomer shift, the average oxidation state of Fe ions in the synthesized titanomagnetite solid solution may be derived from the isomer shift of Fe ions in the room temperature Mössbauer spectra. This method was also employed to identify the oxidation states of Fe ions in iron complexes with cyclam-related ligands [42], a linear relationship between oxidation state of Fe ion and isomer shift was obtained, with oxidation states of Fe ions in the range of 2+ to 6+, and the isomer shift decreasing with the increase in oxidation state. Since the Fe^{3+} and Fe^{2+} ions coexist on either tetrahedral or octahedral site of the synthesized spinel titanomagnetite, the oxidation state of Fe ions derived from the linear relationship (Fig. 4) is not an integer, which in turn reflects the Fe ions distribution. It has been previously confirmed that Ti^{4+} prefers the octahedral site for all of the studied samples and the Fe ion population can be precisely identified from the fits of room temperature Mössbauer spectra. Therefore, we only focus on the isomer shift of Fe ion on the tetrahedral site. If the Fe cation distribution on tetrahedral site is obtained, one can derive the formula of the synthesized titanomagnetite with different molar fraction of ulvöspinel components according to the charge balance. It has to be noted that the effect of possible defects and impurities in the titanomagnetite samples on isomer shifts of Fe ions were not considered.

Due to the strong overlap of Mössbauer sub-spectra it is extremely difficult to figure out the exact percentage of Fe^{2+} and Fe^{3+} ions from the two de-convoluted sextets or doublets on tetrahedral site. Instead, the overall isomer shift of Fe ions on the tetrahedral site was calculated as following, which may reflect more accurate results about the Fe cation distribution:

$$\text{Overall isomer shift of Fe ion} = (\delta_1 A_1 + \delta_2 A_2) / (A_1 + A_2) \quad (3)$$

where δ stands for the isomer shift and A for area percentage of corresponding sub-spectra of Fe ions on tetrahedral site. The calculated overall isomer shifts of Fe ions on the tetrahedral site of titanomagnetite solid solution are shown in Table 2. According to the relationship between isomer shift and oxidation state of Fe ions (Fig. 4), the overall oxidation states of Fe ions on tetrahedral site can be obtained, and the following rules have to be obeyed with:

$$\text{Overall oxidation state of Fe ions} = (+3) \times \text{Fe}_{\text{apfu}}^{3+} + (+2) \times \text{Fe}_{\text{apfu}}^{2+} \quad (4)$$

Table 2Overall isomer shift, oxidation state of Fe ion on tetrahedral site, and the derived site occupancy of titanomagnetite with different ulvöspinel Fe_2TiO_4 components.

x	I.S. (mm/s)	Abund.(%)	Overall I.S. (δ , mm/s)	Overall oxidation state	Derived titanomagnetite formula
0.0	0.059	34.6	0.059	+3	$(\text{Fe}^{3+})[\text{Fe}_1^{2+}\text{Fe}_1^{3+}]\text{O}_4$
	0.472	65.4	0.472*	+2.5*	
0.40	0.191	27.7	0.157	2.88	$(\text{Fe}_{0.88}^{3+}\text{Fe}_{0.12}^{2+})[\text{Fe}_{0.30}^{3+}\text{Fe}_{1.30}^{2+}\text{Ti}_{0.4}^{4+}]\text{O}_4$
	0.071	11.1			
0.60	0.318	29.0	0.324	2.68	$(\text{Fe}_{0.68}^{3+}\text{Fe}_{0.32}^{2+})[\text{Fe}_{0.12}^{3+}\text{Fe}_{1.28}^{2+}\text{Ti}_{0.6}^{4+}]\text{O}_4$
	0.341	11.8			
0.70	0.332	33.4	0.480	2.50	$(\text{Fe}_{0.49}^{3+}\text{Fe}_{0.51}^{2+})[\text{Fe}_{0.11}^{3+}\text{Fe}_{1.19}^{2+}\text{Ti}_{0.7}^{4+}]\text{O}_4$
	0.373	9.8			
0.75	0.772	8.1	0.768	2.16	$(\text{Fe}_{0.005}^{3+}\text{Fe}_{0.995}^{2+})[\text{Fe}_{0.0}^{3+}\text{Fe}_{1.25}^{2+}\text{Ti}_{0.75}^{4+}]\text{O}_4$
	0.768	38.9			
1.0	0.904	50.3	0.904	2	$(\text{Fe}_1^{2+})[\text{Fe}_1^{2+}\text{Ti}_1^{4+}]\text{O}_4$
	0.903	49.7			
Err.	± 0.01	± 0.5	± 0.01	± 0.02	

Note: * 0.472 and +2.5 are the isomer shift and overall oxidation state of Fe ions on octahedral site in magnetite. The titanomagnetite solid solution with $x=0.65$ was not included due to the large amount of impurities.

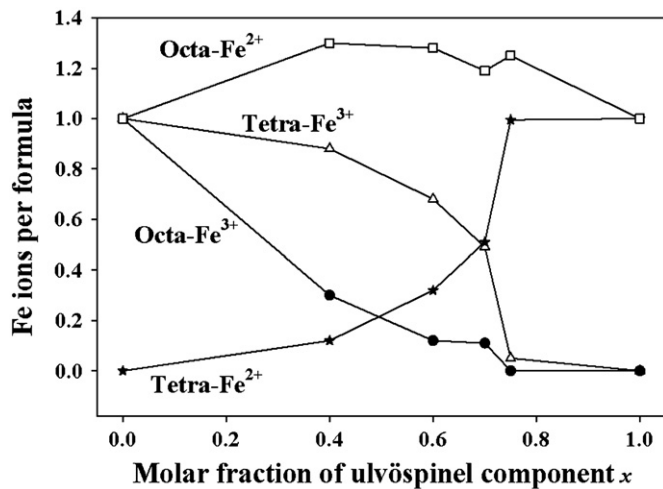


Fig. 5. Cation distribution as a function of molar fraction of ulvöspinel component x in titanomagnetite derived from the relationship between the isomer shift and oxidation states of Fe ions.

and

$$\text{Fe}_{\text{apfu}}^{3+} + \text{Fe}_{\text{apfu}}^{2+} = 1 \quad (5)$$

Here $+3$ and $+2$ are the oxidation states of Fe ions, and $\text{Fe}_{\text{apfu}}^{3+}$ and $\text{Fe}_{\text{apfu}}^{2+}$ are the Fe^{3+} and Fe^{2+} atomic number per formula unit of synthesized titanomagnetite, respectively. The overall isomer shift, overall oxidation state, and derived titanomagnetite formula are summarized in Table 2. The plot of Fe cation distributions as a function of ulvöspinel Fe_2TiO_4 component x is presented in Fig. 5, which is in good agreement with the reported results from O'Reilly et al [11]. It has been reported there are different site occupancy models to describe the Fe^{2+} and Fe^{3+} in titanomagnetite solid solutions [11,14], the difference in those models may arise from differences in synthesis processes, defects, impurities in titanomagnetite solid solution and characterization techniques. Room temperature Mössbauer spectroscopy is another powerful tool to study the cation distribution in titanomagnetite systems.

3.3. Simultaneous DSC–TGA

The thermal behavior of magnetite on heating has been a controversial subject, whether magnetite is oxidized to gamma- Fe_2O_3 or directly to hematite has caused a lot of discussion. For magnetite oxidation, it was summarized that DSC curve gives two

distinct exothermic peaks. The first one was assigned to the oxidation of magnetite to gamma- Fe_2O_3 , while the second corresponds to the change of gamma- Fe_2O_3 to hematite [43]. Recently, the Fe_2TiO_4 – Fe_3O_4 solid solution was studied thermogravimetrically as a function of oxygen activity at high temperature, which provides information on nonstoichiometry and point defects [44]. However, the thermogravimetric behavior of Fe_3O_4 , Fe_2TiO_4 , and the synthesized $x\text{Fe}_2\text{TiO}_4$ – $(1-x)\text{Fe}_3\text{O}_4$ solid solution under inert atmosphere was not studied, despite its importance to understanding the thermal history and magnetic properties of rocks on Mars.

Similar to the oxidation behavior, the DSC curve of the magnetite sample shows two distinguished exothermic peaks and one small endothermic peak (Fig. 6a). The two exothermic peaks are at 534 °C and 647 °C, respectively. The existence of exothermic and endothermic peaks on the DSC curve indicates that magnetite is not stable under heat treatment in inert Ar atmosphere, suggesting there are either some phase transformations or crystallization. The first endothermic phase change occurs below 400 °C with a peak value at 308 °C, while the second exothermic phase change starts at 400 °C with the peak temperature at 534 °C. The third exothermic phase transformation takes place at 570 °C and ends at 700 °C, respectively.

As can be seen in Fig. 6h, the TGA curve of magnetite reveals three major weight losses: one is in the temperature range from 170 °C to 360 °C with a value of $\sim 1.64\%$, and the other starts from 360 °C and ends at 600 °C, with a weight loss of $\sim 0.70\%$. The third weight loss starts at 600 °C and ends at 720 °C, with a value of $\sim 0.20\%$. These three weight losses (with the total weight loss value of $\sim 2.54\%$) have to be due to the decomposition of magnetite. The first weight loss is possibly related to the decomposition of magnetite to non-stoichiometric magnetite, as shown in Eq. (6). The second and the third weight losses at above 360 °C are probably due to the further decomposition of non-stoichiometric magnetite to another type of non-stoichiometric magnetite.



These three weight losses are in good agreement with DSC curves of the original magnetite (Fig. 6a), which shows corresponding endothermic and exothermic peaks.

The DSC–TGA measurement of physically mixed Fe_2TiO_4 – Fe_3O_4 powder (with 1:1 weight ratio) was performed for comparison and was shown in Fig. 7. From the TGA curve of this sample, it was found that the weight loss has a value of $\sim 1.25\%$, which is close to half of the weight loss value of original Fe_3O_4 . The weight loss value for this physically mixed Fe_2TiO_4 – Fe_3O_4 sample is

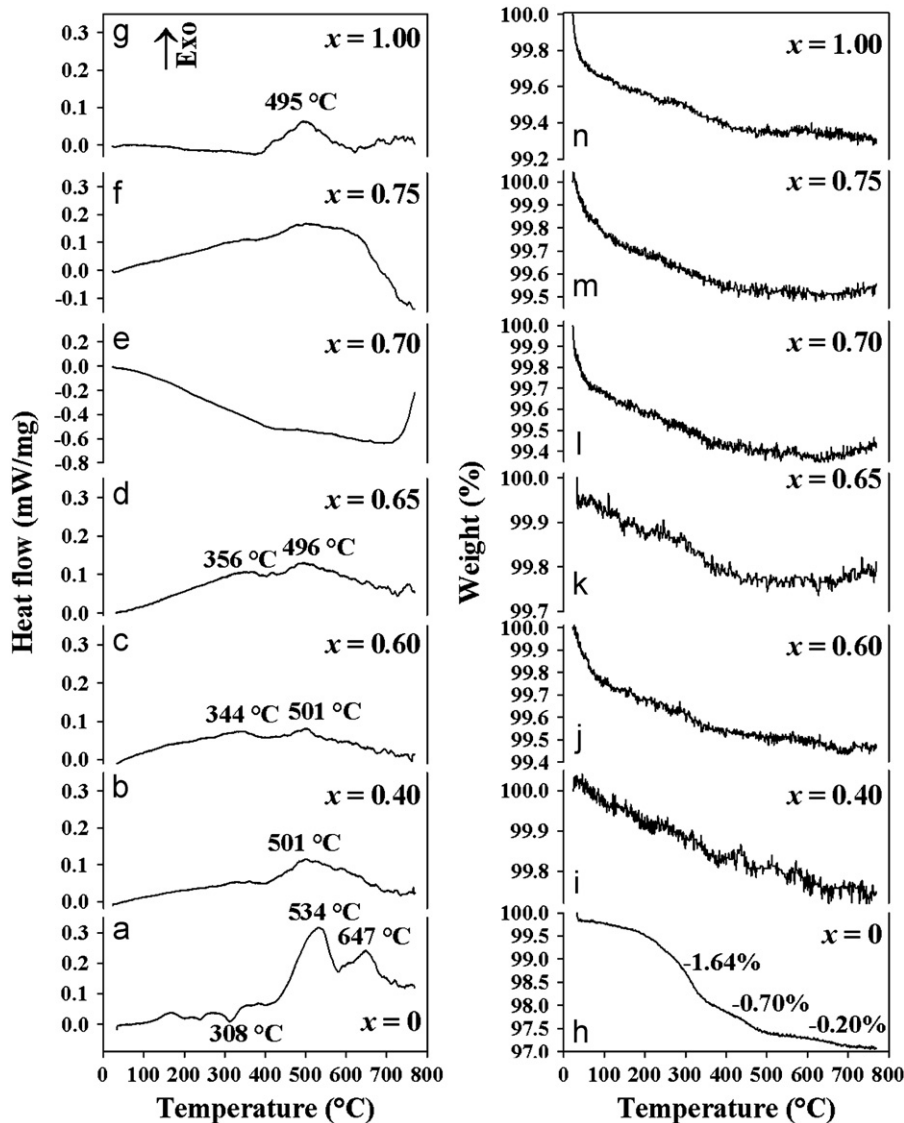


Fig. 6. DSC curves of the $x\text{Fe}_2\text{TiO}_4-(1-x)\text{Fe}_3\text{O}_4$ ($0.4 \leq x \leq 1$) pseudo-binary system with molar fraction x (a) $x=0.0$, (b) $x=0.4$, (c) $x=0.6$, (d) $x=0.65$, (e) $x=0.70$, (f) $x=0.75$ and (g) $x=1.0$, and TGA curves of the $x\text{Fe}_2\text{TiO}_4-(1-x)\text{Fe}_3\text{O}_4$ ($0.4 \leq x \leq 1$) pseudo-binary system with molar fraction x (h) $x=0.0$, (i) $x=0.4$, (j) $x=0.6$, (k) $x=0.65$, (l) $x=0.70$, (m) $x=0.75$ and (n) $x=1.0$.

expected by considering the existence of the Fe_2TiO_4 with a 50% in weight percentage, and also suggests that the decomposition behavior of magnetite is not dramatically affected by the Fe_2TiO_4 . The magnetite will decompose to nonstoichiometric magnetite under heat treatment and this process is completed below 800 °C. However, the DSC curve of this physically mixed $\text{Fe}_2\text{TiO}_4\text{-Fe}_3\text{O}_4$ sample shows totally different behavior as that of original magnetite or Fe_2TiO_4 , as no exothermic peak was observed. Instead, only a broad endothermic peak was observed in the studied temperature range. The observation of one broad endothermic peak and non-existence of exothermic peaks suggests the complicated thermal behavior of the physically mixed $\text{Fe}_2\text{TiO}_4\text{-Fe}_3\text{O}_4$ sample. The overall endothermic behavior may be attributed to the overlap between the decomposition of magnetite and the formation of $\text{Fe}_2\text{TiO}_4\text{-Fe}_3\text{O}_4$ solid solution under heat treatment. It also indicates that the magnetite, even with a low degree of stoichiometry, can also form solid solution with Fe_2TiO_4 under heat treatment.

The DSC-TGA curves of the formed $x\text{Fe}_2\text{TiO}_4-(1-x)\text{Fe}_3\text{O}_4$ solid solution (with $x \geq 0.4$) do not change dramatically, suggesting

that they are thermally stable under heat treatment in Ar atmosphere. The small exothermic peaks on the DSC curves of these samples may be attributed to the crystallization of fine particles. The slight variation in the weight percentages on TGA curves is due to the thermal shift of the weight under heat treatment. The DSC-TGA results are in good agreement with the XRD results that no magnetite phase is detected in the $x\text{Fe}_2\text{TiO}_4-(1-x)\text{Fe}_3\text{O}_4$ solid solution due to the complete consumption of the original magnetite or the non-stoichiometric magnetite.

4. Conclusions

The $x\text{Fe}_2\text{TiO}_4-(1-x)\text{Fe}_3\text{O}_4$ solid solutions with different molar fractions x in the range of $0 \leq x \leq 1$ were successfully synthesized by the use of solid-state reaction. X-ray powder diffraction showed that the synthesized $x\text{Fe}_2\text{TiO}_4-(1-x)\text{Fe}_3\text{O}_4$ systems maintain the inverse spinel structures when Fe ions were replaced by the Ti^{4+} . The lattice parameter a expanded linearly with the increase in the ulvöspinel Fe_2TiO_4 components. ^{57}Fe room

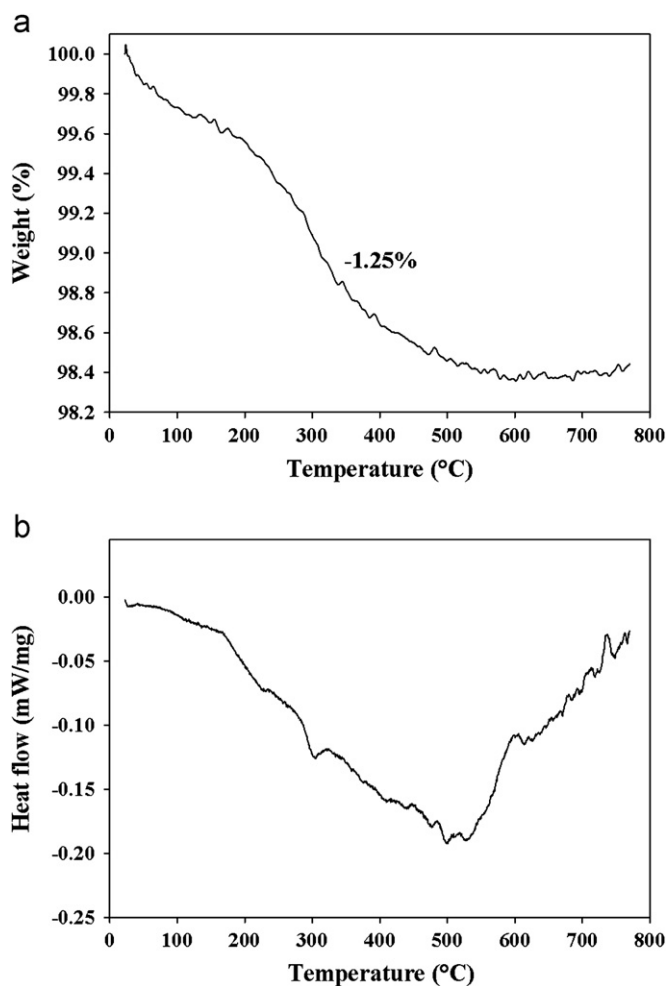


Fig. 7. DSC and TGA curves of physically mixed $\text{Fe}_2\text{TiO}_4\text{-Fe}_3\text{O}_4$ powder with 1:1 ratio in weight percentage: (a) TGA curve and (b) DSC curve.

temperature Mössbauer spectra showed that the magnetic properties of the synthesized solid solutions depend on the molar fraction of Fe_2TiO_4 component x and vary significantly, such that the hyperfine magnetic field decreases with the increase in x value. When x is in the range of $0 \leq x \leq 0.4$, the solid solution shows ferrimagnetic behavior. However, it shows weak ferrimagnetic and paramagnetic behavior with x in the range of $0.4 < x \leq 0.7$. For the solid solution with Fe_2TiO_4 molar fraction $x > 0.70$, it shows paramagnetic behavior, with appearance of only quadrupole doublets in Mössbauer spectra. The accomplishment and significance of this work are that the Fe cation distribution in the synthesized $x\text{Fe}_2\text{TiO}_4\text{-(1-x)Fe}_3\text{O}_4$ systems can be derived from the isomer shift of room temperature Mössbauer spectroscopy. There is a linear relationship between oxidation state of Fe ion and isomer shift, in turn, the overall isomer shift value for Fe ions at tetrahedral sites reflects the overall oxidation state of Fe ions at tetrahedral site, which can be used to determine the Fe cation distribution from the demonstrated method.

The simultaneous differential scanning calorimetry and thermogravimetric analysis (DSC–TGA) showed that magnetite is not stable, and there are some weight losses with exothermic peaks under heat treatment in inert atmosphere due to the decomposition of magnetite to non-stoichiometric magnetite. Magnetite with low degree of stoichiometry can form solid solution with Fe_2TiO_4 . The synthesized solid solution is stable under heat treatment in studied temperature range under Ar atmosphere.

Acknowledgments

The work at Duquesne was supported by the National Science Foundation under grant DMR-0854794.

References

- [1] L.G. Tejuca, J.L. Fireoo, J.M.D. Tascón, Structure and reactivity of perovskite-type oxides, *Advanced Catalysis* 36 (1989) 237–328.
- [2] G. Kletetschka, P.J. Wasilewski, P.T. Taylor, Mineralogy of the source for magnetic anomalies on Mars, *Meteoritics and Planetary Science* 35 (2000) 895–899.
- [3] A. Wise, M. Saenko, A.M. Velázquez, D.E. Laughlin, M. Díaz-Michelena, M.E. McHenry, Phase evolution in the $\text{Fe}_3\text{O}_4\text{-Fe}_2\text{TiO}_4$ pseudo-binary system and its implications for remanent magnetization in Martian minerals, *IEEE Transactions on Magnetics* 47 (2011) 4124–4127.
- [4] R. Sanz, M. Cerdán, M.E. McHenry, M. Díaz-Michelena, Temperature dependent magnetization and remanent magnetization in pseudo-binary $(\text{Fe}_2\text{TiO}_4)_x\text{-(Fe}_3\text{O}_4)_{1-x}$ ($0.30 < x < 1.00$) titanomagnetites, *IEEE Transactions on Magnetics* 47 (2011) 4128–4131.
- [5] E. Schmidbauer, ^{57}Fe Mössbauer spectroscopy and magnetization of cation-deficient Fe_2TiO_4 and FeCr_2O_4 . Part I: ^{57}Fe Mössbauer spectroscopy, *Physics and Chemistry of Minerals* 14 (1987) 533–541.
- [6] E.W. Gorter, Ionic distribution deduced from the g-factor of a ferromagnetic spinel: Ti^{4+} in fourfold co-ordination, *Nature* 173 (1954) 123–124.
- [7] V.A. Bokov, A.S. Kamzin, S.I. Yushchuk, N.N. Parfinova, Magnetic fields at ^{57}Fe nuclei and quadrupole interactions in Ni–Fe–Ti spinels, *Soviet Physics — Solid State* 16 (1975) 2360–2363.
- [8] M.A. Arillo, M.L. López, C. Pico, M.L. Veiga, A. Jiménez, E. Rodriguez-Castellón, Surface characterization of spinels with Ti(IV) distribution in tetrahedral and octahedral sites, *Journal of Alloys and Compounds* 317–318 (2001) 160–163.
- [9] S. Akimoto, Thermo-magnetic study of ferromagnetic minerals contained in igneous rocks, *Journal of Geomagnetism and Geoelectricity* 6 (1954) 1–14.
- [10] L. Néel, Some theoretical aspects of rock magnetism, *Advanced Physics* 4 (1955) 191–242.
- [11] W. O'Reilly, S.K. Banerjee, Cation distribution in titanomagnetites (1–x) $\text{Fe}_3\text{O}_4\text{-x Fe}_2\text{TiO}_4$, *Physics Letters* 17 (1965) 237–238.
- [12] Z. Kakol, J. Sabol, J.M. Honig, Cation distribution and magnetic properties of titanomagnetites $\text{Fe}_{3-x}\text{Ti}_x\text{O}_4$ ($0 \leq x < 1$), *Physical Review B* 43 (1991) 649–654.
- [13] H.H. Hamdeh, K. Barghout, J.C. Ho, P.M. Shand, L.L. Miller, A Mössbauer evaluation of cation distribution in titanomagnetites, *Journal of Magnetism and Magnetic Materials* 191 (1999) 72–78.
- [14] C.I. Pearce, C.M.B. Henderson, N.D. Telling, R.A.D. Patrick, J.M. Charnock, V.S. Coker, E. Arenholz, F. Tuna, G. Van Der Laan, Fe site occupancy in magnetite-ulvöspinel solid solutions: a new approach using X-ray magnetic circular dichroism, *American Mineralogy* 95 (2010) 425–439.
- [15] N. Millot, S.B. Colijn, P. Perriat, G.L. Caër, R. Welter, B. Malaman, Characterization of ferrites synthesized by mechanical alloying and soft chemistry, *Nanostructured Materials* 12 (1999) 641–644.
- [16] D. Basak, J. Ghose, Thermal studies on iron titanate spinel, *Journal of Thermal Analysis* 37 (1991) 935–943.
- [17] A. Roy, J. Ghose, Studies on thermal stability of titanium substituted iron molybdenum spinel oxide, *Journal of Thermal Analysis and Calorimetry* 61 (2000) 839–847.
- [18] P. Ramdohr, Ulvöspinel and its significance in titaniferous iron ores, *Economic Geology* 48 (1953) 677–688.
- [19] M.E. Evans, M.L. Wayman, An investigation of the role of ultra-fine titanomagnetite intergrowth in palaeomagnetism, *Geophysical Journal of the Royal Astronomical Society*, 36 (1974) 1–10.
- [20] P.P.K. Smith, Spinodal decomposition in a titanomagnetite, *American Mineralogy* 65 (1980) 1038–1043.
- [21] L. Végard, Die konstitution der mischkristalle und die raumfüllung der atome, *Zeitschrift für Physik* 5 (1921) 17–26.
- [22] U. Bleil, An experimental study of the titanomagnetite solid solution series, *Pure and Applied Geophysics* 114 (1976) 165–175.
- [23] B.C. Melot, K. Page, R. Seshadri, E.M. Stoudenmire, L. Balents, D.L. Bergman, T. Proffen, Magnetic frustration on the diamond lattice of the A-site magnetic spinels $\text{CoAl}_2\text{-xGa}_x\text{O}_4$: the role of lattice expansion and site disorder, *Physical Review B* 80 (2009) 104420.
- [24] B.A. Wechsler, D.H. Lindsley, C.T. Prewitt, Crystal structure and cation distribution in titanomagnetite ($\text{Fe}_{3-x}\text{Ti}_x\text{O}_4$), *American Mineralogy* 69 (1984) 754–770.
- [25] F. Bosi, U. Hälenius, H. Skogby, Crystal chemistry of the magnetite-ulvöspinel series, *American Mineralogy* 94 (2009) 181–189.
- [26] Y. Nakamura, P.A. Smith, D.E. Laughlin, M. De Graef, M.E. McHenry, Structure and magnetic properties of quenched $(\text{Mn}_x\text{Al}_{1-x})_2\text{O}_4$ spinels and hausmannites, *IEEE Transactions on Magnetics* 31 (1995) 4154–4156.
- [27] Swaminathan, R., McHenry, M.E., Calvin, S., Sorescu, M., Diamandescu, L.: Surface structure model of cuboctahedrally truncated ferrite nanoparticles. Proc. 9th International Conference on Ferrites, American Ceramic Society, pp. 847–852, (2005).

- [28] R. Swaminathan, M.E. McHenry, P. Poddar, H. Srikanth, Magnetic properties of polydisperse and monodisperse NiZn ferrite nanoparticles interpreted in a surface structure model, *Journal Applied Physics* 97 (2005) 10G104.
- [29] R. Swaminathan, J. Woods, S. Calvin, J. Huth, M.E. McHenry, Microstructural evolution model of the sintering behavior and magnetic properties of NiZn ferrite nanoparticles, *Adv. Sci. Tech.* 45 (2006) 2337–2344 Online at <<http://www.scientific.net>>.
- [30] E.J.W. Verwey, P.W. Haayman, Electronic conductivity and transition point of magnetite (Fe_3O_4), *Physica* 8 (1941) 979–987.
- [31] P.W. Readman, W. O'Reilly, S.K. Banerjee, An explanation of the magnetic properties of Fe_2TiO_4 , *Physics Letters A* 25 (1967) 446–447.
- [32] M. Tanaka, T. Tokoro, Y. Aiyama, Jahn–Teller effects on Mössbauer spectra of Fe^{57} in FeCr_2O_4 and FeV_2O_4 , *Journal of the Physical Society of Japan* 21 (1966) 262–267.
- [33] I. Dézsi, I. Szűcs, E. Sváb, Mössbauer spectroscopy of spinels, *Journal of Radioanalytical and Nuclear Chemistry* 246 (2000) 15–19.
- [34] R. Vanleerberghe, R.E. Vandenberghe, Determination of the quadrupole splitting distributions of the A and B-site ferrous ions in Fe_2TiO_4 , *Hyperfine Interactions* 23 (1985) 75–87.
- [35] W. Lowrie, *Fundamentals of Geophysics*, 1st edition, Cambridge University Press, Cambridge, UK, 1997 243.
- [36] H. Tanaka, M. Kono, Mössbauer spectra of titanomagnetite: a reappraisal, *Journal of Geomagnetism and Geoelectricity* 39 (1987) 463–475.
- [37] K. Melzer, Z. Šimša, M. Łukasiak, J. Suwalski, Mössbauer spectra and electronic properties of titanomagnetite, *Crystal Research and Technology* 22 (1987) K132–K136.
- [38] N. Guigue-Millot, Y. Champion, M.J. Hÿtch, F. Bernard, S. Bégin-Colin, P. Perriat, Chemical heterogeneities in nanometric titanomagnetites prepared by soft chemistry and studied ex situ: evidence for Fe-segregation and oxidation kinetics, *Journal of Physical Chemistry B* 105 (2001) 7125–7132.
- [39] S.K. Banerjee, W. O'Reilly, T.C. Gibb, N.N. Greenwood, The behaviour of ferrous ions in iron-titanium spinels, *Journal of Physics and Chemistry of Solids* 28 (1967) 1323–1335.
- [40] P. Nagarajan, C.K.R. Murty, Mössbauer and magnetic studies on the system of $\text{Fe}_{3-x}\text{Ti}_x\text{O}_4$, *Bulletin of Materials Science* 3 (1981) 217–224.
- [41] L.R. Walker, G.K. Werthim, V. Jaccarino, Interpretation of the Fe^{57} isomer shift, *Physical Review Letters* 6 (1961) 98–101.
- [42] J.F. Berry, E. Bill, E. Bothe, S.D. George, B. Mienert, F. Neese, K. Wieghardt, An octahedral coordination complex of iron (VI), *Science* 312 (2006) 1937–1941.
- [43] K.V.G.K. Gokhale, Study on the oxidation of magnetite, *Economic Geology* 56 (1961) 963–971.
- [44] S. Aggarwal, R. Dieckmann, Point defects and cation tracer diffusion in $(\text{Ti}_x\text{Fe}_{1-x})_{3-\delta}\text{O}_4$ 1. Non-stoichiometry and point defects, *Physics and Chemistry of Minerals* 29 (2002) 695–706.